

By Rodney C. Wingrove and Robert E. Coate
Research Scientists

NASA, Ames Research Center, Moffett Field, Calif.

Summary

This paper presents an analysis of a guidance method which uses a reference trajectory. The four state variables needed to prescribe the trajectory are used as follows: Velocity is made the independent variable, and the errors in the rate-of-climb, acceleration, and range variables away from the reference are used to govern the lift. A linearized form of the motion equations is used to show that this represents a third-order control system. First- and second-order control terms (rate of climb and acceleration inputs) are shown to determine the entry corridor depth by stabilizing the trajectory so that the vehicle does not skip back out of the atmosphere or does not exceed a specified acceleration limit. The destabilizing effect that range input (the third-order control term) can have is illustrated and the results indicate that a low value of range input gain must be used at the high supercircular velocities while larger values of range input gain can be used at lower velocities.

The usable corridor depth and range capability with this guidance system are demonstrated for a lifting capsule ($L/D = 0.5$). The practical applications of this system are illustrated with a fixed trim configuration wherein roll angle is used to command the desired lift. The results show that the guidance system requires only one reference trajectory for abort entry conditions as well as for entry conditions near the design values.

Introduction

Current and future manned space flight projects require the development of entry guidance methods applicable to blunt-shaped vehicles entering the earth's atmosphere at supercircular velocities. These guidance systems must regulate small lift changes in such a manner that constraints, such as acceleration and heating, are not exceeded and that the vehicle arrives at a predetermined destination. Various entry guidance and control methods which meet some or all of these needs have been considered¹⁻¹³ and although these studies do present solutions to the problem, they do not analyze in detail the control parameters which strongly influence the entry guidance system. It is the purpose of this paper to demonstrate, by means of control system analysis techniques, the influence of various control parameters upon the trajectory motion. A simple guidance method, using a reference trajectory, will be developed from these principles, and a linearized form of the entry motion equations will be used to describe mathematically the trajectory dynamics resulting from this guidance method.

This guidance technique will be demonstrated for entries of a low-lift ($L/D = 0.5$, $W/C_D S = 48$ psf) vehicle with entrance conditions (a velocity of 36,000 ft/sec at an altitude of 400,000 ft) that are to be expected in the return from a lunar mission. As previously shown^{14,15} the entrance velocity requires that lift be varied in such a manner that it does not let the vehicle skip out of the atmosphere or exceed a given acceleration limit.

The use of lift variations to keep the vehicle within these constraints will be studied and the manner in which range must be controlled to reach a desired endpoint will be considered. Finally, as a practical application, the control system is illustrated with a fixed-trim configuration in which roll angle is used to control lift during entry. The guidance characteristic of this system is shown for entries from a lunar mission as well as for entries at possible abort conditions.

Control System Analysis

Dynamics of Entry Motion

In order to study the dynamics of entry motion a set of equations is needed which not only describes the important aspects of the motion but which also has simple analytical solutions for use with control system analysis techniques. The equations of motion in the plane of the trajectory in their standard form - two second-order nonlinear differential equations with time as the independent variable - can only be solved by a computer and they do not, as such, lend themselves to a general analytical solution. Chapman¹⁶ has shown that these equations may be approximated by one second-order nonlinear differential equation with normalized velocity, \bar{u} , as the independent variable. Although his equation does indicate the important control aspects in entry motion, its nonlinear nature does not allow the use of standard control system analysis techniques. Before the Chapman equation can be used to analyze the trajectory motion, it must be linearized. The linearization given in the appendix will be used throughout this paper to illustrate the effects of various trajectory parameters that might be used to govern lift variation.

Fig. 1(a) shows a block diagram of the linearized equation of motion derived in the appendix. The equation of motion is a second-order differential equation in either altitude, acceleration, or temperature along the trajectory. However, when range is considered, the equation becomes a third-order differential equation. To illustrate the dynamics graphically in terms of the variation of trajectory parameters with velocity, \bar{u} , a simplified representation of the motions at the bottom of skip is shown in Fig. 1(b). When the altitude, acceleration, and temperature are near a maximum (or minimum) their corresponding rates of change must, of course, change sign. Also near this point, the range curve has an inflection point. The curves on Fig. 1(b) indicate graphically the integrations (1/s) shown in the block diagram.

It is interesting to note the loops inherent in the motion equation shown in Fig. 1. The upper loop, $(1 - \bar{u}^2)/A^2$, corresponds to the spring constant of the second-order differential equation, and, therefore, it determines the natural frequency of the trajectory oscillation. This loop is stabilizing when velocity, \bar{u} , is less than 1 (local circular velocity), but it is destabilizing when velocity is greater than 1. The lower loop, $1/\bar{u}$, is a first-order damping term that adds damping to the trajectory oscillations.

*Presented at the IAS National Meeting, St. Louis, Missouri, April 30 - May 2, 1962.

This simplified representation of the dynamics gives some insight into the terms a lift control system should incorporate. For instance, lift variation controlled by range measurements represents a third-order system. It can be reasoned that this third-order system, like any other classical third-order control system, needs first- and second-order feedback terms for satisfactory dynamic response. The first-order term in this case is represented by the rate of change of altitude, acceleration, or temperature and the second-order term can be represented by the value of altitude, acceleration, or temperature. It appears that simple entry control techniques can be conceived by consideration of these system dynamics. One method which will be demonstrated here is the guidance about a stored reference trajectory. The system chosen uses the difference in range from that of the reference trajectory as the third-order feedback term, with errors in acceleration and in rate of climb used as second- and first-order feedback terms. The command equation for lift-drag ratio is

$$L/D = (L/D)_{ref} + K_1\dot{\Delta h} + K_2\Delta A + K_3\Delta R$$

where $(L/D)_{ref}$ is the L/D function used to describe the reference trajectory, and the error quantities, Δh , ΔA , and ΔR , are the difference between measured variables and the stored reference variables as a function of the velocity, \bar{u} , along the trajectory. A block diagram of this control system is shown in Fig. 2.

The trajectory dynamics associated with each of the feedback terms in this control system will be shown. Comparison of the trajectory motions resulting from simulated controlled trajectories will be made with the linearized analytical expression of the motion taken from the appendix. The use of first- and second-order terms (\dot{h} , A) to control the trajectory and thus assure a satisfactory corridor depth will first be discussed. Then the manner in which the third-order range term must be used will be demonstrated and the maximum value of downrange and crossrange available will be determined.

Design Reference Trajectory

The reference trajectory to be used must be precomputed for the desired path through the atmosphere to the desired touchdown. The entrance conditions for the reference trajectory are limited to those within the safe entry corridor. This corridor, which can be defined in terms of possible initial entrance angles, is presented in Fig. 3 in relation to the overshoot boundary, where the vehicle will just stay within the atmosphere, and the undershoot boundary, where the vehicle will reach a specified deceleration limit. The reference trajectory is computed for a prescribed L/D variation which gives the desired path through the atmosphere. In this report the computed reference trajectory is expressed as an L/D function proportional to rate of climb.

$$(L/D)_{ref} = K_1\dot{h}_{ref}$$

Fig. 4 shows typical trajectories obtained when L/D is controlled by a constant-gain ($K_1 = -0.001/\text{fps}$) feedback for various initial entry angles. With this program for L/D the maximum value of L/D is commanded for the initial portion of the entry; L/D is then varied, as the

function of rate of climb, to stabilize the trajectory; and, finally, at subcircular velocities, about half of the maximum L/D available is commanded, thus giving a trajectory within the center of the subcircular maneuvering capability of the vehicle. The reference trajectories in Fig. 4 have a particular variation of rate of climb, acceleration, and range with respect to velocity which can be used for the reference values in the complete control equation

$$L/D = (L/D)_{ref} + K_1\dot{\Delta h} + K_2\Delta A + K_3\Delta R$$

The $(L/D)_{ref}$ is that L/D used to describe the reference trajectory, $(L/D)_{ref} = K_1\dot{h}_{ref}$. A simplification can be made in this equation by noting that with this particular reference trajectory

$$(L/D)_{ref} + K_1\dot{\Delta h} = K_1\dot{h}_{ref} + K_1(\dot{h} - \dot{h}_{ref}) = K_1\dot{h}$$

so that the equation reduces to

$$L/D = K_1\dot{h} + K_2\Delta A + K_3\Delta R$$

Trajectories, also shown in Fig. 4, represent limiting values for the constraints used in this study. The overshoot trajectory ($\gamma_1 = -4.6^\circ$) defines the skipout limit since the maximum negative lift, in this case $L/D = -0.5$, fails to keep the vehicle within the atmosphere. The steepest entrance angle $\gamma_1 = -7.5^\circ$ shown in Fig. 4 is determined by the acceleration limit ($-10g$) which is a function of the maximum acceleration force that can be tolerated by the vehicle or crew. The $-10g$ acceleration limit is shown¹⁷ to be a realistic value for humans. The effect of the permissible acceleration level on the corridor boundary will be demonstrated.

Control System With Acceleration and Rate-of-Climb Inputs

The effects of the various feedback quantities upon the entry trajectory can be shown by using the input quantities independently and in combination. The first quantity to be considered is acceleration feedback which is used to control L/D in the following manner,

$$L/D = (L/D)_{ref} + K_2\Delta A$$

Fig. 5 shows trajectories for various entry conditions where L/D was controlled only by the acceleration error. It can be seen in Fig. 5 that the resulting trajectories are very oscillatory about the reference trajectory. The oscillatory character of this control is to be expected because, as was pointed out earlier, the acceleration feedback is of second order and would thus modify the frequency, but not the damping, in the equation of motion.

Since the trajectories are highly oscillatory when only acceleration feedback is used, it would seem reasonable that the addition of rate of climb, which is essentially a first-order feedback quantity, will damp the motions. The combined acceleration and rate-of-climb trajectory control is specified by the following equation

$$L/D = (L/D)_{ref} + K_1\dot{\Delta h} + K_2\Delta A$$

This method of control is illustrated in Fig. 6 wherein the acceleration error ΔA is shown versus

velocity for various constant K_1 gains in the trajectory control equation. The effect of the rate-of-climb control is particularly evident in this figure because, as can be seen from the curves, when the K_1 gain is increased, the resulting vehicle acceleration damps quite rapidly to the acceleration profile of the reference trajectory. When rate-of-climb feedback gain is approximately $-0.001/\text{fps}$, the damping, as can be seen in Fig. 6, is almost critical and the vehicle acceleration reaches the design trajectory acceleration with a small amount of overshoot by the time the vehicle velocity has decreased to local circular velocity ($\bar{u} = 1$).

An approximate analytical description of the trajectory dynamics for this combined rate of climb and acceleration feedback can be obtained from the linearized equations in the appendix. From the appendix the linearized characteristic equation with combined rate of climb and acceleration feedback is

$$s^2 + \left(\frac{1}{\bar{u}} - 25,800K_1\right)s + 900 \left(\frac{1 - \bar{u}^2}{A_{\text{ref}}^2} - K_2\right) = 0$$

from this equation

$$2\zeta\omega_n = \frac{1}{\bar{u}} - 25,800K_1, \text{ (radians/unit of } \bar{u}\text{)}$$

and

$$\omega_n^2 = 900 \left(\frac{1 - \bar{u}^2}{A_{\text{ref}}^2} - K_2\right), \text{ (radians/unit of } \bar{u}\text{)}^2$$

If K_1 and K_2 are set equal to zero, these expressions for damping and frequency reduce to the values inherent in equations of motion with no L/D variations. It can be seen that if K_1 and K_2 are negative numbers, they will increase the damping and the frequency of the trajectory oscillations. If, for example, we set $K_1 = -0.001/\text{fps}$, $K_2 = -0.33/g$ at $\bar{u} = 1$, the computed damping factor is $\zeta = 0.78$. The corresponding curve of Fig. 6 compares favorably with this result. The approximate formulas for damping and natural frequency can be seen to give a quantitative as well as a qualitative insight into the effect of the rate-of-climb and acceleration gains upon the vehicle trajectory.

Typical rate-of-climb and acceleration-controlled trajectories are shown in Fig. 7 for various initial entry angles. It can be seen that for the usable range of entry angles, the vehicle trajectory damps to the reference trajectory by the time the vehicle velocity has decreased to approximately local circular velocity.

Usable Corridor Depth

The limits of entrance angle within which a specific vehicle will enter the atmosphere without violating any of the constraints placed upon its trajectory determine the usable corridor depth. A comparison is made in Fig. 8 of the usable corridor depth for the three control combinations considered thus far. From Fig. 8 it is seen that with L/D variation controlled by combined acceleration and rate of climb, the usable corridor depth is almost equal to the available corridor depth. When L/D variation is controlled by acceleration errors, the usable corridor depth is approximately 10 miles less than the available corridor depth regardless of the acceleration constraint placed upon the

trajectory. When L/D is controlled only by rate of climb, the usable corridor depth is about 13 miles less than that available. The data in Fig. 8 represent the maximum usable corridor depths to be expected with the given K_1 and K_2 gains. The usable corridor is primarily a function of the first- and second-order feedback terms. Additional effects of range, the third-order feedback term, upon the trajectory characteristics will next be considered.

Control System With Range Input

A control system using range measurements in a fashion that will assure the vehicle's arrival at a desired destination at the end of the reentry is prescribed in the following manner:

$$L/D = (L/D)_{\text{ref}} + K_1\Delta\dot{h} + K_2\Delta A + K_3\Delta R$$

or, for the particular case considered herein,

$$L/D = K_1\dot{h} + K_2\Delta A + K_3\Delta R$$

The range error term, ΔR , is the difference between range to the destination and range the reference trajectory will traverse. If this error is zero by the end of the trajectory, then the vehicle will reach its destination. The terms $K_1\Delta\dot{h}$ and $K_2\Delta A$ are those described in the previous sections and are used to give acceptable control of L/D.

The effect of range input gain, K_3 , is shown in Fig. 9 for a given initial range error about a given reference trajectory. Using a low value of gain does not correct entirely the range error by the end of the trajectory. On the other hand, large values of range input gain will overcontrol the vehicle and can cause it to skip out as shown in the figure. In order to gain a better understanding of the problem, an approximate analytical expression for the trajectory dynamics derived in the appendix can be used to assess the effect of range-error gain. From the appendix the linearized motion equation at local points along the trajectory can be stated:

$$s^3 + \left(\frac{1}{\bar{u}} - 25,800K_1\right)s^2 + 900 \left(\frac{1 - \bar{u}^2}{A_{\text{ref}}^2} - K_2\right)s + \frac{3.6 \times 10^8 \bar{u}}{A_{\text{ref}}^2} K_3 = 0$$

This is a linear third-order equation and the standard methods of control analysis can be used to gain insight into the trajectory dynamics. One simple method of analysis is to determine the values of K_3 which make this equation stable. From Routh's criterion for stability, K_3 must be positive and also

$$K_3 < \frac{\left(\frac{1 - \bar{u}^2}{A_{\text{ref}}^2} - K_2\right) \left(\frac{1}{\bar{u}} - 25,800K_1\right) A_{\text{ref}}^2}{4,000 \bar{u}}$$

The above expression can be used to determine the upper limit on K_3 (i.e., the upper limit based on stability consideration) and can be used to observe the qualitative interaction of K_1 , K_2 , K_3 , and \bar{u} on trajectory stability. From the above equation, increasing the magnitude of K_1 and K_2 will allow the upper limit on K_3 to increase and it is

important to note that the upper limit of K_3 will increase as \bar{u} decreases. To maximize range capability and drive the range error to zero by the end of the trajectory it is desirable to have a large value of range input gain, K_3 , but still maintain a margin of system stability. This value of gain must be small, then, when \bar{u} is large (i.e., $\bar{u} > 1$) and larger values of gain can only be used when \bar{u} is small (i.e., $\bar{u} < 1$).

The maneuvering longitudinal range capability boundaries as a function of initial entry angle that result from various range input techniques are presented in Fig. 10. In this figure the range of the reference trajectory is 3400 miles and rate-of-climb feedback gain and acceleration feedback gain are held constant. The curves labeled range input from $\bar{u} \approx 1$ were obtained with $K_3 = 0$ when $\bar{u} > 1$ and $K_3 = 0.006/\text{mile}$ when $\bar{u} < 1$, and the curves labeled "range input" from $\bar{u} = 1.4$ mean that $K_3 = 0.0008/\text{mile}$ when $\bar{u} > 1$ and $K_3 = 0.006/\text{mile}$ when $\bar{u} < 1$. It can be seen that if range control is exerted only when velocity is less than local circular velocity, the vehicle has a range capability of approximately 2000 miles for any entry angle within the usable entry corridor. In contrast, when two-step range input is used from $\bar{u} = 1.4$ the range capability is increased 500 to 2000 miles, depending upon the initial entry angle. However, for shallow entry angles and for flight ranges greater than the reference trajectory, there is an approximate 6-mile reduction in the usable entry corridor. This is because, if for shallow-entry angles an attempt is made to extend range when $\bar{u} > 1$, the range input will overpower the first- and second-order input terms and cause the vehicle to skip out. Even though there is this slight loss in usable corridor depth, this use of a small range input gain at the higher velocity adds considerably more usable range.

The attainable ground area for two different corridors is shown in Figs. 11(a) and 11(b). The conics in these figures represent the vacuum trajectories for the extreme entry angles at the boundaries of the corridor in each case and the shaded areas represent the ground area that can be reached from any entry angle within the corridor. In Fig. 11(a) for the 34-mile usable entry corridor depth between $\gamma_1 = -5.3^\circ$ and $\gamma_1 = -7.5^\circ$ the attainable ground area is about 2200 miles of downrange capability and from ± 250 to ± 350 miles of crossrange capability. In Fig. 11(b) for the 11-mile usable entry corridor depth between $\gamma_1 = -5.8^\circ$ and $\gamma_1 = -6.5^\circ$ the attainable ground area for the vehicle is 3900 miles downrange and ± 250 to ± 550 miles crossrange. These data illustrate the trade off that must be considered between the specified corridor depth and attainable ground area. This demonstrates that the largest ground area can be attained if the entry can be made within the smallest specified corridor. These data also show the capabilities that can be expected for the supercircular entries. The following section illustrates the application of these control-system principles to a particular vehicle.

Control-System Application

The control-system principles described in this study will now be demonstrated by application to a particular entry vehicle. The vehicle chosen is a lifting capsule configuration trimmed by center-of-gravity position to give a constant angle

of attack that produces a ratio of 0.5 between the force normal to flight path and the drag force along the flight path. The vehicle roll angle is then used to control the lift force in the vertical plane during entry. This roll-angle command method will be illustrated for entries from a lunar mission, as well as for entries from abort conditions.

Roll-Angle Command

The control method described in this study is used merely to null errors in the trajectory variables. It is therefore reasonable to expect that the full transformation that relates roll angle to L/D [$L/D = (L/D)_{\text{max}} \cos \phi$] need not be used in the command equation. Instead, the following simplified command equation, which was found to be adequate, will be used.

$$|\phi| - 90^\circ = K_1' \dot{h} + K_2' \Delta A + K_3' \Delta R$$

The predetermined reference trajectory that is needed for this control system is computed by controlling a trajectory with $|\phi| - 90^\circ = K_1' \dot{h}$ exactly as was done in the previous section. During an entry, the $K_1' \dot{h}$ and $K_2' \Delta A$ terms in the command equation cause the vehicle trajectory to converge to the design trajectory; the range input term, $K_3' \Delta R$, can be used to null the range error so that the vehicle reaches a prescribed destination. In the command equation a low value of range gain, K_3' , is used when vehicle velocity is greater than local circular velocity. Larger values of range gain, compatible with the previous stability considerations, are used when vehicle velocity is less than local circular velocity.

The command equation determines the magnitude of the roll angle, and the sign of the roll angle is determined by crossrange. The method of determining the sign of the command roll angle by crossrange to the destination is shown in Fig. 12. The method is to let the vehicle fly to one side until the crossrange to the destination exceeds a value specified by a design envelope at which time the sign of the roll-angle command is reversed. The allowable crossrange design envelope is made a function of \bar{u}^2 which is shown¹⁸ to be a good approximation for crossrange capability of a vehicle, particularly when its speed is less than local circular velocity. For the control system used here the crossrange to the destination is allowed to become equal to approximately one-half ($100 \bar{u}^2$, miles) the maximum crossrange capability of the vehicle, at which time the sign of the roll-angle command is reversed. This procedure usually entails a maximum of four to six roll reversals during typical entry trajectories.

Entry From Lunar Trajectory

Both automatic and piloted control have been studied for this type of roll-angle command system. Fig. 13 shows a typical trajectory in which roll angle is controlled by the automatic system. It can be seen that the crossrange error becomes zero by the end of the trajectory, and the downrange error, which is initially -1500 miles, converges to zero at the end of the trajectory. The attainable ground area and usable corridor depth obtained with this roll command system is essentially the same as given by Fig. 10, where a similar 3400-mile design trajectory was used. It is important to note that this range capability is achieved with one design

Notation

A	horizontal acceleration, g units
C_D	drag coefficient, $\frac{D}{(1/2)\rho V^2 S}$
D	drag force, lb
g	local gravitational acceleration, ft/sec ²
\dot{h}	rate of climb, fps
K_1, K_2, K_3	gain constants
L	lift force, lb
m	mass of vehicle, slugs
r	distance from planet center, ft
R	downrange value along a local great circle route in space, miles
S	surface area, ft ²
u	circumferential velocity component normal to radius vector, fps
\bar{u}	dimensionless ratio, $\frac{u}{\text{circular orbital velocity}}, \frac{u}{\sqrt{gr}}$
V	resultant velocity, fps
W	weight of vehicle, lb
β	atmospheric density decay parameter, ft ⁻¹
γ	flight path angle relative to local horizontal; positive for climb
ρ	atmosphere density, slugs/cu ft
ϕ	roll angle, deg
ζ	damping factor
ω_n	natural frequency, $\frac{\text{radian}}{\text{unit of } \bar{u}}$

Subscripts

ref	respect to reference trajectory
1	initial value

References

1. Eggleston, John M., and Young, John W.: Trajectory Control for Vehicles Entering the Earth's Atmosphere at Small Flight-Path Angles. NASA TR R-89, 1961.
2. Creer, Brent Y., Heinle, Donovan R., and Wingrove, Rodney C.: Study of Stability and Control Characteristics of Atmospheric-Entry Type Aircraft Through Use of Piloted Flight Simulators. Paper no. 59-129, Inst. Aero. Sci., 1959.
3. Cheatham, Donald C., Young, John W., and Eggleston, John M.: The Variation and Control of Range Traveled in the Atmosphere by a High-Drag Variable-Lift Entry Vehicle. NASA TN D-230, 1960.
4. Assadourian, Arthur, and Cheatham, Donald C.: Longitudinal Range Control During the Atmospheric Phase of a Manned Satellite Reentry. NASA TN D-253, 1960.
5. Foudriat, Edwin C.: Study of the Use of a Terminal Controller Technique for Reentry Guidance of a Capsule-Type Vehicle. NASA TN D-828, 1961.
6. Young, John W.: A Method for Longitudinal and Lateral Range Control for a High-Drag Low-Lift Vehicle Entering the Atmosphere of a Rotating Earth. NASA TN D-954, 1961.
7. Lowry, James H., Jr., and Buehrle, Clayton D.: Guidance and Control of Point Return Vehicles. Proc. Nat. Specialists Meeting on Guidance of Aerospace Vehicles (Boston, Mass.), Inst. Aero. Sci., May 1960, pp. 28-33.
8. White, J. A., Foudriat, E. C., and Young, J. W.: Guidance of a Space Vehicle to a Desired Point on the Earth's Surface. Preprint no. (61-41) American Astronautical Soc., Jan. 1961.
9. Wingrove, Rodney C., and Coate, Robert E.: Piloted Simulator Tests of a Guidance System Which Can Continuously Predict Landing Point of a Low L/D Vehicle During Atmosphere Re-entry. NASA TN D-787, 1961.
10. Wingrove, Rodney C., and Coate, Robert E.: Piloted Simulation Studies of Re-entry Guidance and Control at Parabolic Velocities. Paper no. 61-195-1889, Inst. Aero. Sci., 1961.
11. Dow, Paul C., Jr., Fields, Donald P., and Scammell, Frank H.: Automatic Re-entry Guidance at Escape Velocity. Preprint no. 1946-61, American Rocket Society, 1961.
12. Bryson, Arthur E., and Denham, Walter F.: A Guidance Scheme for Supercircular Re-entry of a Lifting Vehicle. ARS Space Flight Report to the Nation, Oct. 1961.
13. Morth, Raymond, and Speyer, Jason: Control System for Supercircular Entry Maneuvers. IAS Paper No. 62-3, Jan. 1962.
14. Chapman, Dean R.: An Analysis of the Corridor and Guidance Requirements for Supercircular Entry Into Planetary Atmospheres. NASA TR R-55, 1960.
15. Wong, Thomas J., and Slye, Robert E.: The Effect of Lift on Entry Corridor Depth and Guidance Requirements for the Return Lunar Flight. NASA TR R-80, 1961.
16. Chapman, Dean R.: An Approximate Analytical Method for Studying Entry Into Planetary Atmospheres. NASA TR R-11, 1959.

The operator transform of equation (4) may be written: (Note that \bar{u} in eq. (1) is negative during solution of an entry trajectory.)

$$\left[s^2 + \frac{1}{\bar{u}} s + \frac{\beta r(1 - \bar{u}^2)}{A_{ref}^2} \right] \Delta Z = - \frac{\sqrt{\beta r} \Delta(L/D)}{\bar{u}} \quad (5)$$

The dynamics of this characteristic equation will be described for various functions controlling $\Delta(L/D)$.

Rate-of-Climb Input

The expression for rate of climb in the Z function notation¹⁸ is $\dot{h} = \sqrt{g/\beta} (\bar{u}Z' - Z)$, fps; L/D is controlled by \dot{h} errors about the reference trajectory in the following manner:

$$\Delta(L/D) = K_1 \Delta \dot{h} = K_1 \sqrt{g/\beta} (\bar{u} \Delta Z' - \Delta Z)$$

This $\Delta(L/D)$ can be substituted into equation (4) to obtain the following result:

$$s^2 + \left(\frac{1}{\bar{u}} - K_1 \sqrt{gr} \right) s + \frac{\beta r(1 - \bar{u}^2)}{A_{ref}^2} - \frac{K_1 \sqrt{gr}}{\bar{u}} = 0$$

Then at each local point along the trajectory, the damping and natural frequency can be approximated by:

$$2\zeta\omega_n \approx \frac{1}{\bar{u}} - K_1 \sqrt{gr}, \text{ radians/unit of } \bar{u}$$

$$\omega_n^2 \approx \frac{\beta r(1 - \bar{u}^2)}{A_{ref}^2} - \frac{K_1 \sqrt{gr}}{\bar{u}}, \text{ (radians/unit of } \bar{u})^2$$

From these approximate solutions, important features of the dynamics can be noted. The gain K_1 must be negative to increase the damping of the trajectory and this in turn increases the natural frequency. The increase in ω_n^2 is very slight, however, for the K_1 large enough to give near critical damping ($\zeta = 1$); so then rate of climb is essentially a simple first-order feedback term, that is, affecting the damping only. In future derivations the K_1 contribution to natural frequency will be omitted.

Acceleration Input

The expression for acceleration in the Z function notation¹⁸ is $A = -\sqrt{\beta r} \bar{u}Z$, g. Acceleration errors control L/D about the reference trajectory in the following manner:

$$\Delta(L/D) = K_2 \Delta A = -K_2 \sqrt{\beta r} \bar{u} \Delta Z$$

This value $\Delta(L/D)$ can be substituted into equation (4) to obtain:

$$s^2 + \frac{1}{\bar{u}} s + \beta r \left(\frac{1 - \bar{u}^2}{A_{ref}^2} - K_2 \right) = 0$$

At each local point along the trajectory, the dynamics may be approximated by:

$$2\zeta\omega_n \approx \frac{1}{\bar{u}}, \text{ radians/unit of } \bar{u}$$

$$\omega_n^2 \approx \beta r \left(\frac{1 - \bar{u}^2}{A_{ref}^2} - K_2 \right), \text{ (radians/unit of } \bar{u})^2$$

It is apparent then that if K_2 is negative, the natural frequency is increased and K_2 will not affect the damping.

Range Input

The expression for range in the Z function notation¹⁸ is

$$R = \frac{r}{5280 \sqrt{\beta r}} \int_{\bar{u}_2}^{\bar{u}_1} \frac{d\bar{u}}{Z}, \text{ miles}$$

The L/D is controlled by range errors about the reference trajectory in the following manner:

$$\begin{aligned} \Delta \frac{L}{D} &= K_3 \Delta R \\ &= K_3 \frac{r}{5280 \sqrt{\beta r}} \left[\int_{\bar{u}_2}^{\bar{u}_1} \frac{(Z_{ref} - \Delta Z) d\bar{u}}{(Z_{ref} - \Delta Z)(Z_{ref} + \Delta Z)} \right. \\ &\quad \left. - \int_{\bar{u}_2}^{\bar{u}_1} \frac{d\bar{u}}{Z_{ref}} \right] \end{aligned}$$

If ΔZ^2 is neglected compared to Z_{ref}^2 this becomes

$$\Delta \frac{L}{D} = -K_3 \frac{r}{5280 \sqrt{\beta r}} \int_{\bar{u}_2}^{\bar{u}_1} \frac{\Delta Z}{Z_{ref}^2} d\bar{u}$$

This value of $\Delta(L/D)$ may be substituted into equation (4) and the equation becomes

$$s^3 + \frac{1}{\bar{u}} s^2 + \frac{\beta r(1 - \bar{u}^2)}{A_{ref}^2} s + \frac{\beta r^2 \bar{u} K_3}{5280 A_{ref}^2} = 0$$

For this third-order equation not to have a positive root, K_3 must be greater than zero and \bar{u} must be less than unity. An upper limit for K_3 may be determined by using Routh's criterion for stability; that is, the trajectory will be stable if

$$K_3 < \frac{1 - \bar{u}^2}{\bar{u}^2} \left(\frac{5280}{r} \right)$$

As is shown in the text, other inputs (i.e., accelerations and rate-of-climb control) will add damping to the control system and permit a larger value of K_3 than the one shown here for range error input alone.

trajectory. If greater ranges are required than those shown in Fig. 10, another design trajectory will have to be used. The range capability is essentially the same for either automatic or piloted control because under normal conditions the task of following the command roll angle can be accomplished by either with nearly equal facility. However, the pilot will strongly influence the successful completion of an entry mission when an emergency situation occurs. For instance, simulation studies with NASA test pilots indicate that this particular roll-angle control task can be accomplished even when the short-period stability augmentation system fails.

Entry From Abort Trajectories

The possibility of an abort during a lunar mission poses the most stringent requirement that can be placed upon a guidance system - that it be able to cope with those conditions which are extremely far from the design trajectory. Typical abort trajectories were flown using this roll command guidance system and are shown in Fig. 14. These trajectories represent reentries at 26,000 ft/sec and 32,000 ft/sec where the destination is 1,500 miles from entry into the atmosphere. Many extreme abort conditions were investigated. The sensitive situation for this guidance system, and one which would be difficult for most guidance methods, was found to be emergency entry in which the vehicle at the bottom of the first skip is near circular velocity and range extension is needed from this point to reach the destination. The entry at 26,000 fps in Fig. 14 illustrates such a sensitive situation. Although these entry conditions are quite different from the reference trajectory, the guidance system is able to govern the trajectory so that the vehicle reaches its destination and none of the acceleration constraints are violated.

The ability of this control system, which uses only one reference trajectory, to handle these off-design entrance conditions is due primarily to the fact that the four state variables needed to describe the trajectory are contained in the guidance law. This is equivalent to the fact that all three of the feedback loops are used in the third-order control system described as a function of velocity. This control system therefore is able to damp out the oscillations along the trajectory and guide the vehicle to a desired end point.

Conclusions

It has been shown in this paper that reentry-trajectory control systems can be represented as a third-order control system described with respect to velocity. The first- and second-order feedback terms determine the vehicle's usable corridor depth because they damp the vehicle trajectory to the reference trajectory in such a way that the vehicle does not skip out of the atmosphere or exceed specified acceleration limits. Range error feedback, the third-order term of the control system, must have a high gain at velocities less than local circular velocity to insure that range errors are zero by the end of the trajectory, and the feedback gain must be low at higher velocities to insure trajectory stability.

A system using one reference trajectory was investigated for a low L/D vehicle and super-circular entry velocities. The results indicate

that for a 34-mile usable corridor depth, attainable downrange increment is on the order of 2200 miles, and for an 11-mile usable corridor depth, attainable downrange increment is on the order of 3900 miles.

This reference trajectory system was demonstrated for a lifting capsule configuration where roll angle is varied to modulate lift. The control system using only one reference trajectory gives satisfactory guidance for entries from design super-circular velocities as well as entries from abort or emergency conditions.

Appendix

An approximate equation that represents the dynamics of the equations of motion about a reference trajectory can be derived by a linearization of the following Chapman equation¹⁶

$$Z'' - \frac{Z'}{\bar{u}} + \frac{Z}{\bar{u}^2} - \frac{1 - \bar{u}^2}{\bar{u}^2 Z} = - \frac{\sqrt{\beta r} (L/D)}{\bar{u}} \quad (1)$$

where

$$Z = \frac{\rho \bar{u}}{2(m/C_D S)} \sqrt{\frac{r}{\beta}}$$

Z' and Z'' are the first and second derivatives with respect to \bar{u} .

Let $\Delta Z''$, $\Delta Z'$, and ΔZ denote the variations of the vehicle trajectory from a reference trajectory; then equation (1) can be written in the following form:

$$\begin{aligned} (Z''_{\text{ref}} + \Delta Z'') - \frac{1}{\bar{u}}(Z'_{\text{ref}} + \Delta Z') + \frac{Z_{\text{ref}} + \Delta Z}{\bar{u}^2} \\ - \frac{1 - \bar{u}^2}{\bar{u}^2 (Z_{\text{ref}} + \Delta Z)} \left(\frac{Z_{\text{ref}} - \Delta Z}{Z_{\text{ref}} - \Delta Z} \right) = - \frac{\sqrt{\beta r} (L/D)}{\bar{u}} \end{aligned} \quad (2)$$

Now if this equation is linearized by neglecting $(\Delta Z)^2$ compared to Z_{ref}^2 , it becomes:

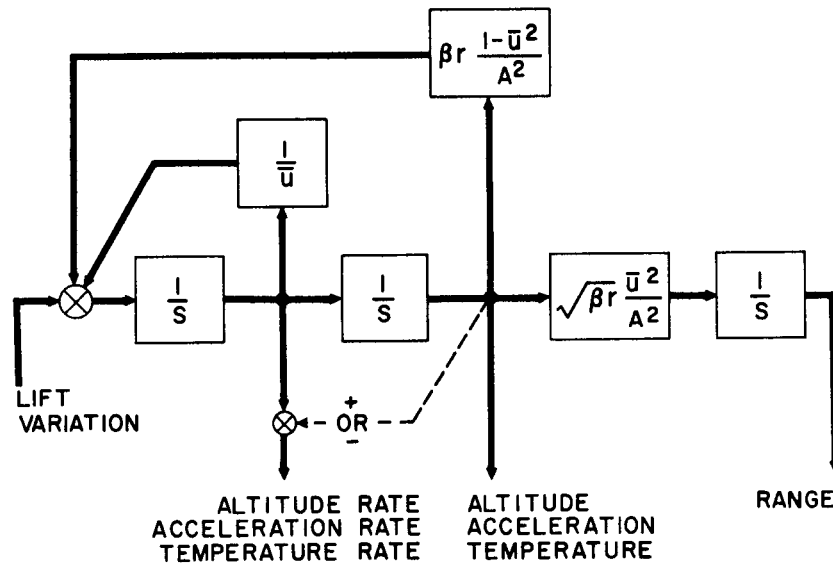
$$\begin{aligned} \Delta Z'' - \frac{\Delta Z'}{\bar{u}} + \left(\frac{1}{\bar{u}^2} + \frac{1 - \bar{u}^2}{\bar{u}^2 Z_{\text{ref}}^2} \right) \Delta Z \\ = -Z''_{\text{ref}} + \frac{Z'_{\text{ref}}}{\bar{u}} - \left(\frac{1}{\bar{u}^2} - \frac{1 - \bar{u}^2}{\bar{u}^2 Z_{\text{ref}}^2} \right) Z_{\text{ref}} - \frac{\sqrt{\beta r} (L/D)}{\bar{u}} \end{aligned} \quad (3)$$

This is a linear differential equation in ΔZ with variable coefficients. The left side is the "characteristic equation" that describes oscillations of the trajectory about the reference trajectory defined by the right side of equation (3) when $L/D = (L/D)_{\text{ref}}$. Then when $L/D = (L/D)_{\text{ref}}$ the right side of the equation is the Chapman equation, (1), for the reference trajectory and may be set equal to zero.

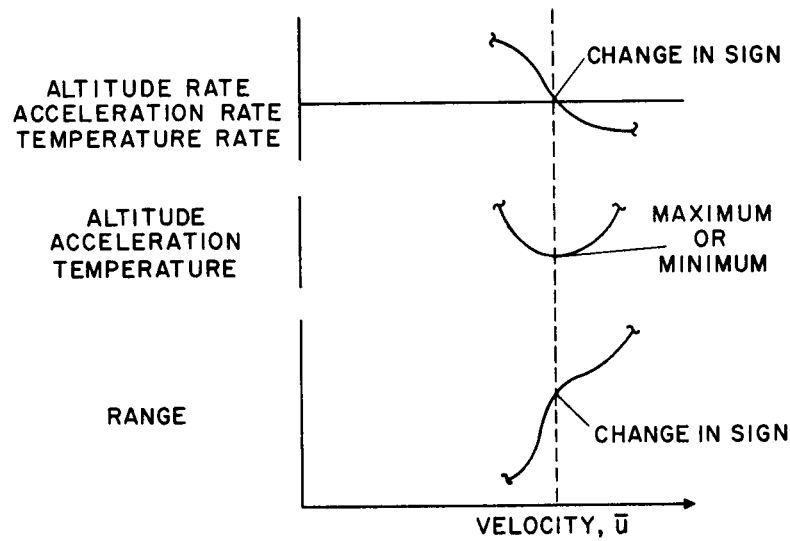
By noting that $-\sqrt{\beta r} \bar{u} Z_{\text{ref}} = A_{\text{ref}}$ and that $1/\bar{u}^2$ is small compared to $(1 - \bar{u}^2)/(\bar{u}^2 Z_{\text{ref}}^2)$, equation (3) may be written:

$$\Delta Z'' - \frac{\Delta Z'}{\bar{u}} + \frac{\beta r (1 - \bar{u}^2)}{A_{\text{ref}}^2} \Delta Z = - \frac{\sqrt{\beta r} \Delta(L/D)}{\bar{u}} \quad (4)$$

17. Creer, Brent Y., Smedal, Harald A., Capt. USN (MC), and Wingrove, Rodney C.: Centrifuge Study of Pilot Tolerance to Acceleration and the Effects of Acceleration on Pilot Performance. NASA TN D-337, 1960.
18. Slye, Robert E.: An Analytical Method for Studying the Lateral Motion of Atmosphere Entry Vehicles. NASA TN D-325, 1960.



(a) Linearized form of entry motion.



(b) Typical dynamics in entry motion.

Fig. 1.- Dynamics of entry motion.

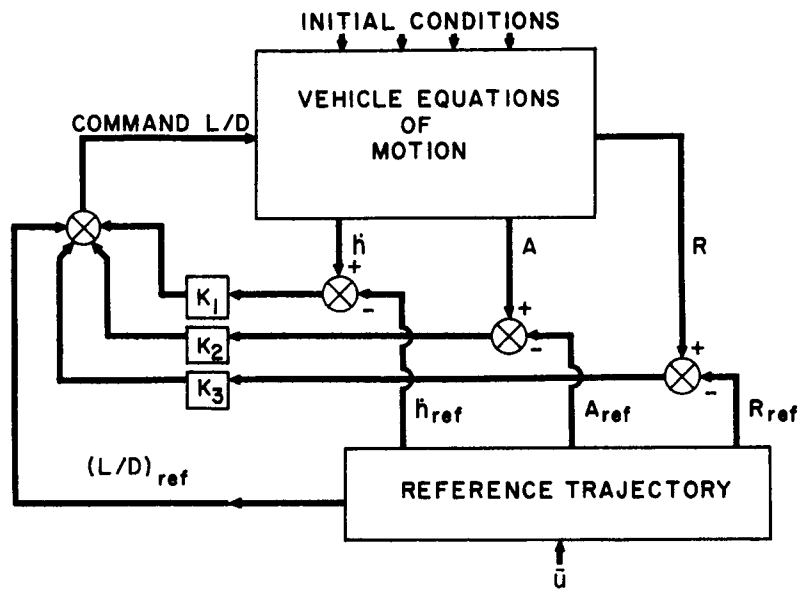


Fig. 2.- Block diagram of reference-trajectory control system.

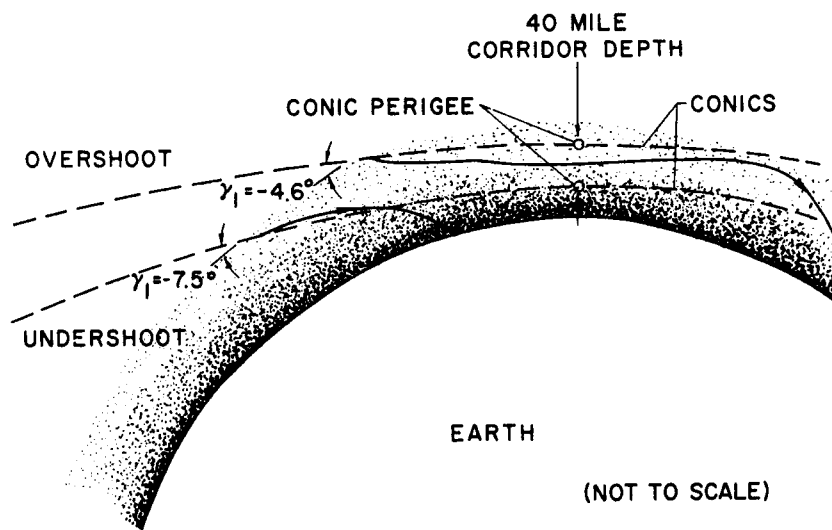


Fig. 3.- Definition of corridor depth.

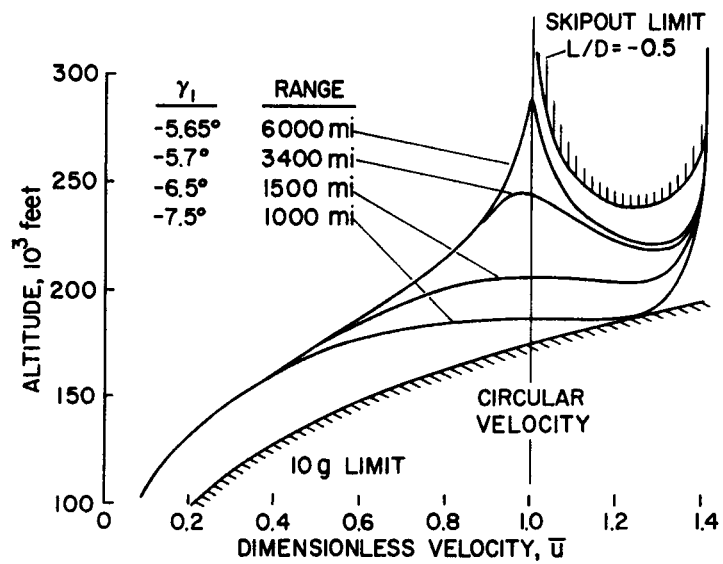


Fig. 4.- Entry trajectories controlled with rate-of-climb input;
 $K_1 = -0.001/\text{fps}$.

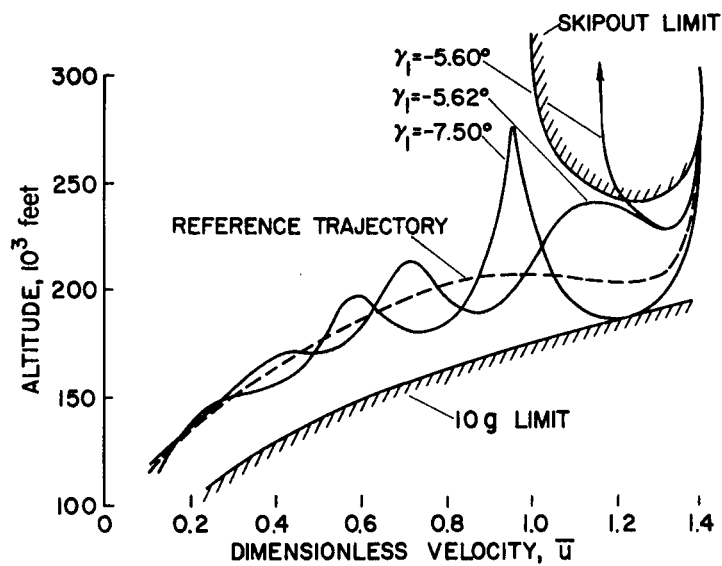


Fig. 5.- Acceleration input used for control about the reference trajectory with design of $\gamma_1 = -6.5^\circ$; $K_2 = -0.33/g$.

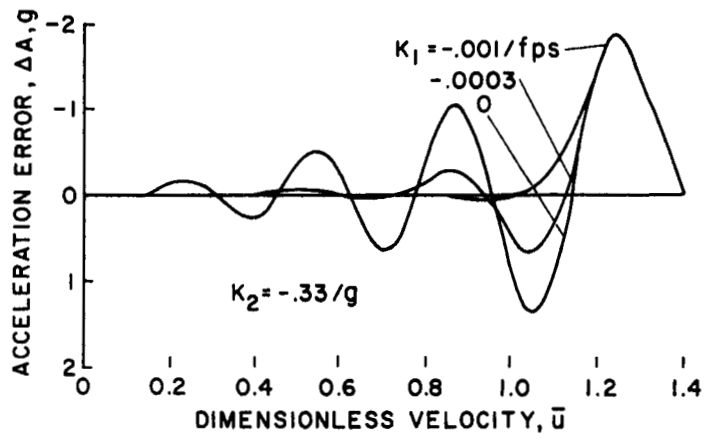


Fig. 6.- Effect of control gain on acceleration errors about the reference trajectory with design $\gamma_1 = -6.5^\circ$; $\gamma_1 = -7^\circ$.

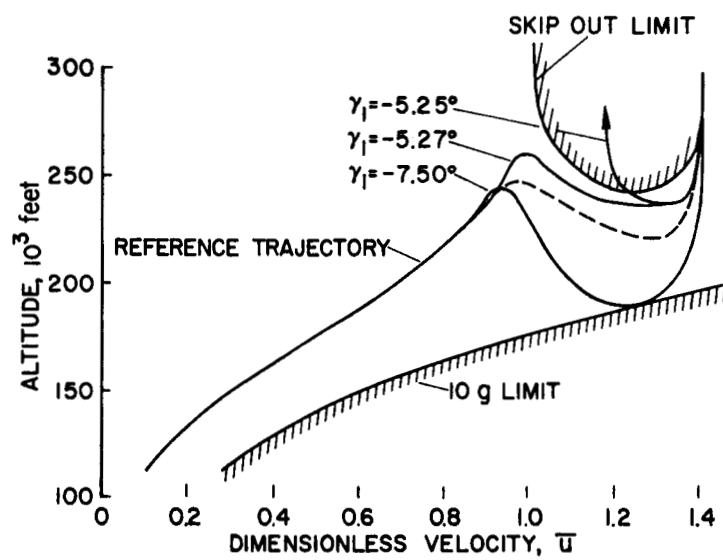


Fig. 7.- Combined acceleration and rate-of-climb inputs used for control about the reference trajectory with design $\gamma_1 = -5.7^\circ$; $K_1 = -0.001/fps$; $K_2 = -0.33/g$.

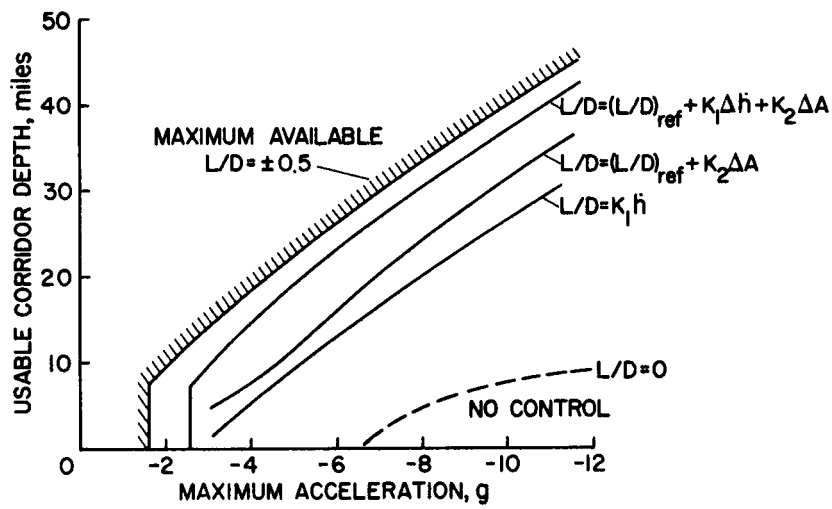


Fig. 8.- Usable corridor depth for various methods of controlling L/D ;
 $K_1 = -0.001/\text{fps}$; $K_2 = -0.33/g$.

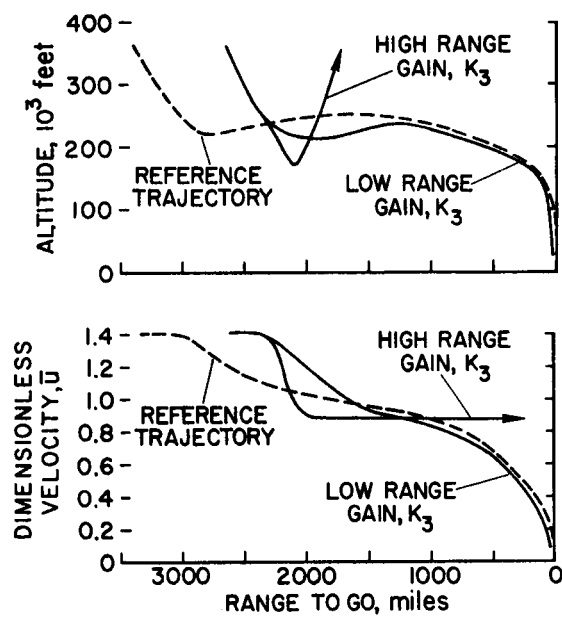


Fig. 9.- Effect of range input gain on the controlled trajectory with
 design range to go = 3400 miles; range to go = 2500 miles; $\gamma_1 = -5.7^\circ$;
 $K_1 = -0.001/\text{fps}$; $K_2 = -0.33/g$; $K_3 = 0.0008$ and $0.006/\text{mile}$.

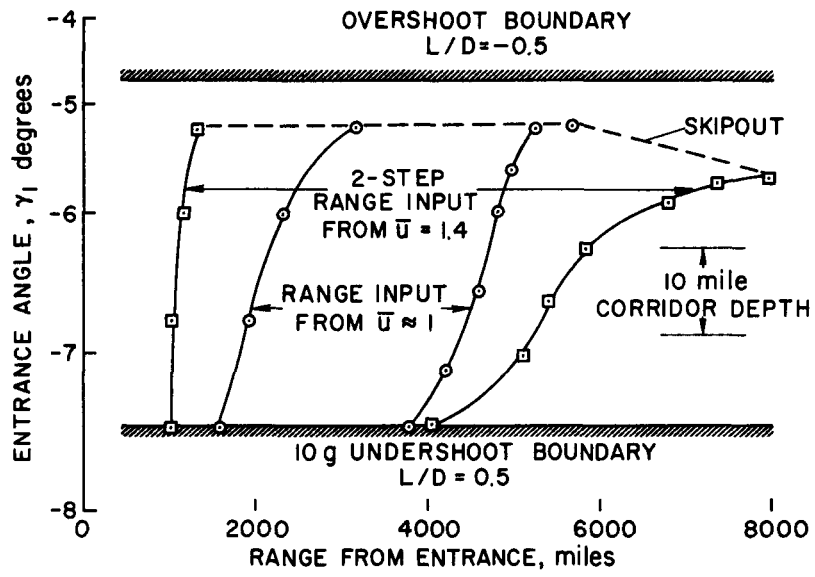
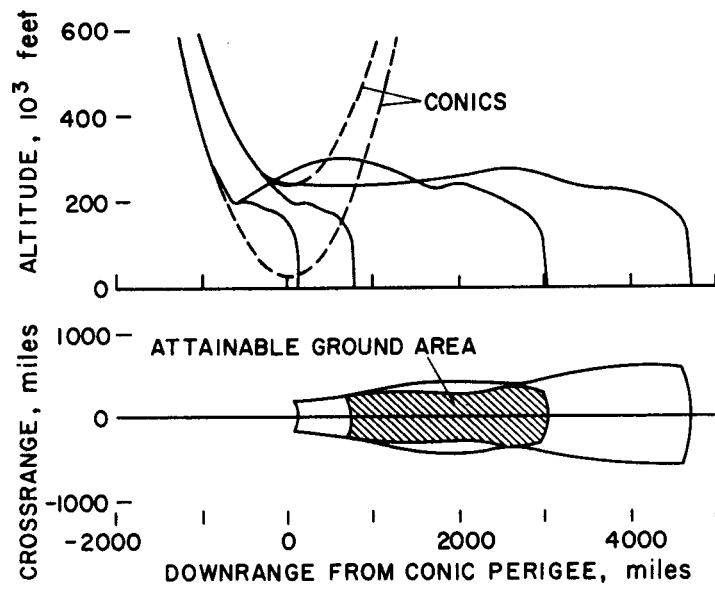
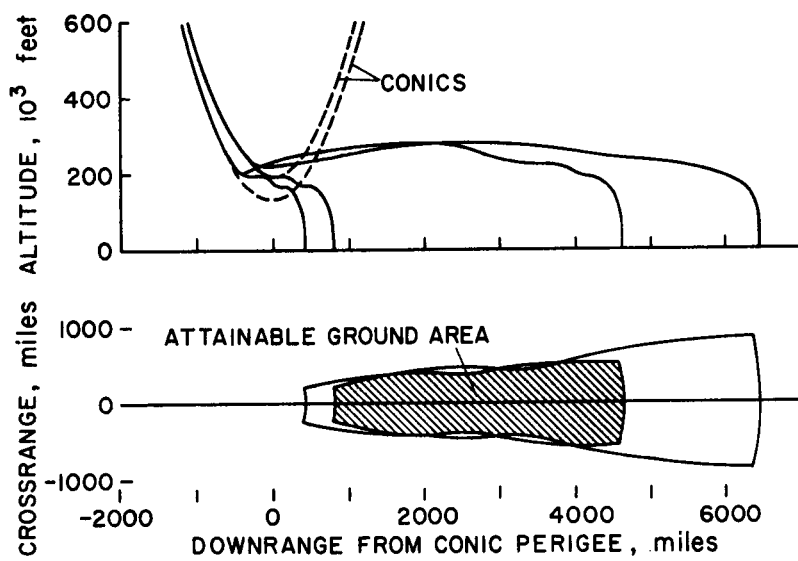


Fig. 10.- Downrange capability as a function of entrance angle for the 3400 mile design trajectory; $K_1 = -0.001/\text{fps}$; $K_2 = -0.33/\text{g}$; $K_3 = 0.0008$ and $0.006/\text{mile}$.



(a) $\gamma_1 = -5.3^\circ$ and -7.5° ; 34-mile usable corridor depth.



(b) $\gamma_1 = -5.8^\circ$ and -6.5° ; 11-mile usable corridor depth.

Fig. 11.- Attainable ground area for various combinations of entrance angle using the 3400-mile design reference trajectory.

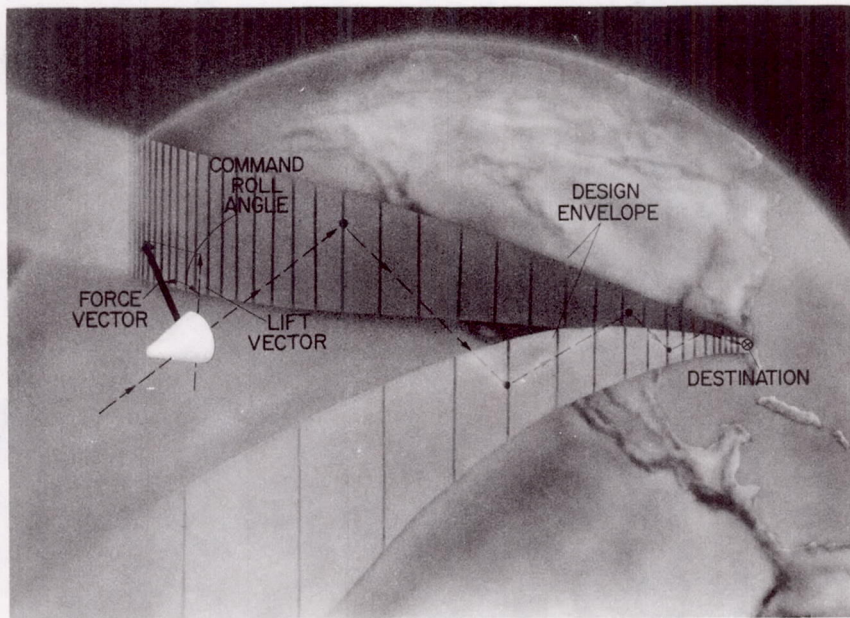


Fig. 12.- Method of crossrange control for lifting capsule.

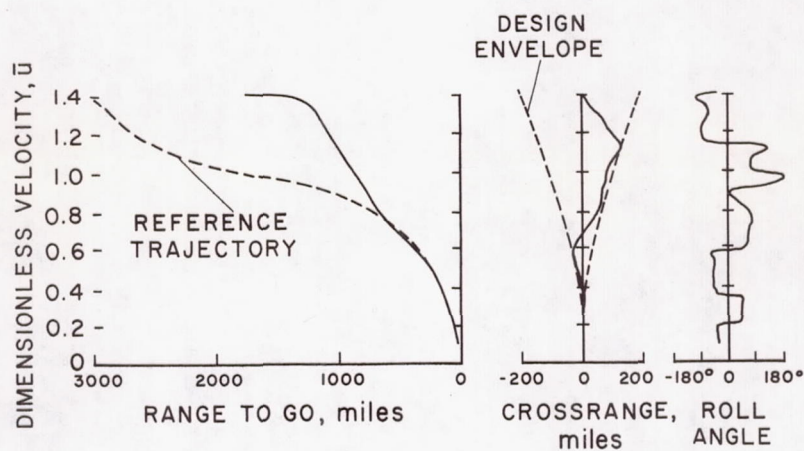
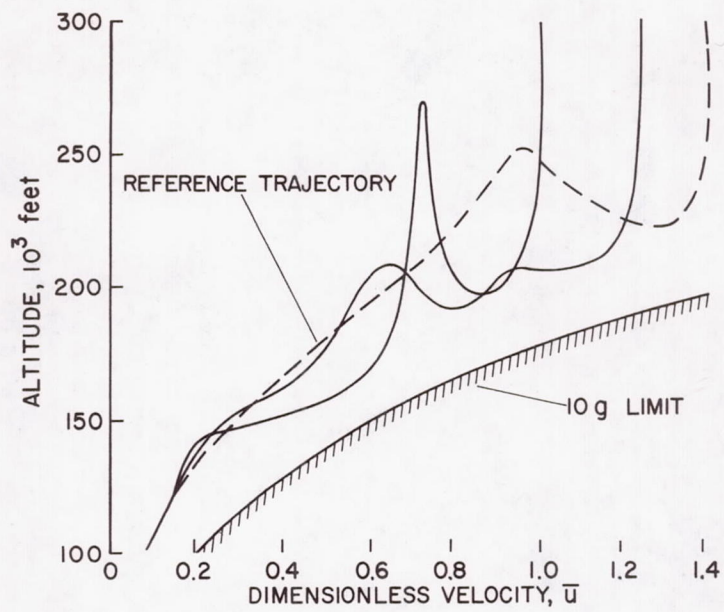
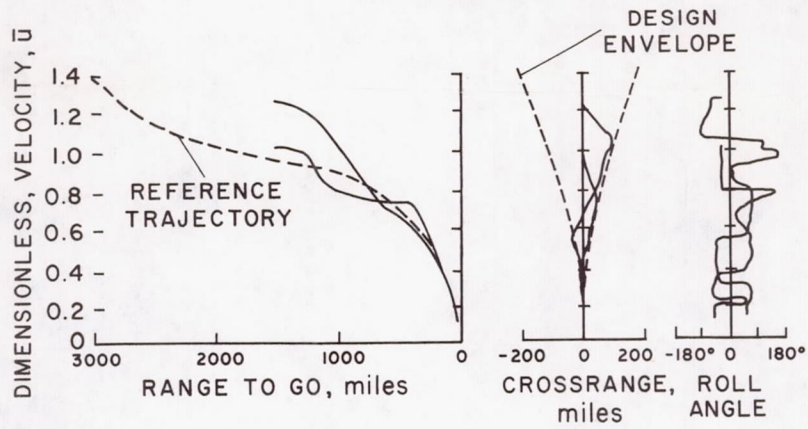


Fig. 13.- Trajectory controlled by roll-angle command; $V_1 = 36,000$ fps;
 $h_1 = 400,000$ feet; $\gamma_1 = -5.8^\circ$; range to go = 1,700 miles;
 design range to go = 3,400 miles.



(a) Altitude variation with velocity.



(b) Downrange, crossrange, and roll-angle variations.

Fig. 14.- Abort trajectories controlled by roll-angle command; $V_1 = 26,000$ and $32,000$ fps; $h_1 = 300,000$ feet; $\gamma_1 = -4^\circ$; range to go = $1,500$ miles; design range to go = $3,400$ miles at $36,000$ fps.

LIFT CONTROL DURING ATMOSPHERE ENTRY FROM SUPERCIRCULAR VELOCITY

By Rodney C. Wingrove and Robert E. Coate

Captions

Fig. 1.- Dynamics of entry motion. (a) Linearized form of entry motion. (b) Typical dynamics in entry motion.

Fig. 2.- Block diagram of reference-trajectory control system.

Fig. 3.- Definition of corridor depth.

Fig. 4.- Entry trajectories controlled with rate-of-climb input; $K_1 = -0.001/\text{fps}$.

Fig. 5.- Acceleration input used for control about the reference trajectory with design of $\gamma_1 = -6.5^\circ$; $K_2 = -0.33/\text{g}$.

Fig. 6.- Effect of control gain on acceleration errors about the reference trajectory with design $\gamma_1 = -6.5^\circ$; $\gamma_1 = -7^\circ$.

Fig. 7.- Combined acceleration and rate-of-climb inputs used for control about the reference trajectory with design $\gamma_1 = -5.7^\circ$; $K_1 = -0.001/\text{fps}$; $K_2 = -0.33/\text{g}$.

Fig. 8.- Usable corridor depth for various methods of controlling L/D; $K_1 = -0.001/\text{fps}$; $K_2 = -0.33/\text{g}$.

Fig. 9.- Effect of range input gain on the controlled trajectory with design range to go = 3400 miles; range to go = 2500 miles; $\gamma_1 = -5.7^\circ$; $K_1 = -0.001/\text{fps}$; $K_2 = -0.33/\text{g}$; $K_3 = 0.0008$ and $0.006/\text{mile}$.

Fig. 10.- Downrange capability as a function of entrance angle for the 3400-mile design trajectory; $K_1 = -0.001/\text{fps}$; $K_2 = -0.33/\text{g}$; $K_3 = 0.0008$ and $0.006/\text{mile}$.

Fig. 11.- Attainable ground area for various combinations of entrance angle using the 3400-mile design reference trajectory. (a) $\gamma_1 = -5.3^\circ$ and -7.5° ; 34-mile usable corridor depth. (b) $\gamma_1 = -5.8^\circ$ and -6.5° ; 11-mile usable corridor depth.

Fig. 12.- Method of crossrange control for lifting capsule.

Fig. 13.- Trajectory controlled by roll-angle command; $V_1 = 36,000 \text{ fps}$; $h_1 = 400,000 \text{ feet}$; $\gamma_1 = -5.8^\circ$; range to go = 1,700 miles; design range to go = 3,400 miles.

Fig. 14.- Abort trajectories controlled by roll-angle command; $V_1 = 26,000$ and $32,000 \text{ fps}$; $h_1 = 300,000 \text{ feet}$; $\gamma_1 = -4^\circ$; range to go = 1,500 miles; design range to go = 3,400 miles at 36,000 fps. (a) Altitude variation with velocity. (b) Downrange, crossrange, and roll-angle variations.